Please provide feedback

Please support the ScholarWorks@UMBC repository by emailing scholarworks-group@umbc.edu and telling us what having access to this work means to you and why it's important to you. Thank you.

Pulse propagation, dispersion, and energy in magnetic materials

Michael Scalora,[1] Giuseppe D'Aguanno,[2] Nadia Mattiucci,[2,3] Neset Akozbek,[2] Mark J. Bloemer,[1] Marco Centini,[4] Concita Sibilia,[4] and Mario Bertolotti[4]

[1]*Charles M. Bowden Research Center, AMSRD-AMR-WS-ST, RDECOM, Redstone Arsenal, Alabama 35898-5000, USA*
[2]*Time Domain Corporation, Cummings Research Park, 7057 Old Madison Pike, Huntsville, Alabama 35806, USA*
[3]*Università "Roma Tre," Dipartimento di Fisica "E. Amaldi," Via Della Vasca Navale 84, I-00146 Rome, Italy*
[4]*INFM at Dipartimento di Energetica-Universita' di Roma "La Sapienza"-Via Scarpa 16 00161 Roma, Italy*

We discuss pulse propagation effects in generic, electrically and magnetically dispersive media that may display large material discontinuities, such as a surface boundary. Using the known basic constitutive relations between the fields, and an explicit Taylor expansion to describe the dielectric susceptibility and magnetic permeability, we derive expressions for energy density and energy dissipation rates, and equations of motion for the coupled electric and magnetic fields. We then solve the equations of motion in the presence of a single interface, and find that in addition to the now-established negative refraction process an energy exchange occurs between the electric and magnetic fields as the pulse traverses the boundary.

PACS number(s): 42.25.Bs, 42.25.Gy, 78.20.Ci

I. INTRODUCTION

During the past few years, the study of magnetically active, negative index materials (NIMs) [1–3] has led many researchers to reevaluate and characterize a number of many well-known electromagnetic propagation phenomena as they occur in NIMs. For example, many workers have reported on different aspects of the dynamics involving NIMs that range from causality [4] and superluminal propagation [5], to two-dimensional propagation that includes material dispersion [6]. Other subjects tackled include wave-front distortions of steady state transverse Gaussian beams [7], modification of quantum mechanical spontaneous and stimulated emission rates [8], multilayer NIM stacks [9], nonlinear interactions [10], and propagation in guiding layers surrounded by NIM [11]. More recently, gap solitons [12] and optical diode-like [13] behavior have also been predicted.

The dynamics of short pulses (i.e., at least two-dimensional wave packets having finite spatial and temporal width, not infinitely long sources or wires that carry sinusoidal currents) undergoing negative refraction has previously been reported in the linear regime using the matrix transfer method [14,15]. However, many issues relating to the dynamics of pulse propagation still remain unresolved. For example, the issue of energy, energy flow, and energy redistribution within a NIM is an open question, just as it is for ordinary positive index materials [16,17]. A modified energy density had already been derived for dispersive ε and μ, but under conditions of relative transparency (negligible absorption) and the quasimonochromatic regime [16,18]:

$$U(z,t) = \frac{1}{8\pi}\left[\mathrm{Re}\left(\frac{\partial[\omega\varepsilon(\omega)]}{\partial\omega}\right)|\mathbf{E}|^2 + \mathrm{Re}\left(\frac{\partial[\omega\mu(\omega)]}{\partial\omega}\right)|\mathbf{H}|^2\right].$$

(1)

Under conditions of normal dispersion, away from resonances, Eq. (1) insures that energy remains positive [16], but it is believed to fail whenever absorption is an important component of the dynamics [19], as in plasmas [20], or met-

als, for example. A simple inspection of Eq. (1) reveals that it also fails under conditions of anomalous dispersion, i.e., in proximity of resonances and large absorption. Although Eq. (1) appears to have limited validity [5,21], we will show that it can still be used for pulses only a few wave cycles in duration, *under conditions of normal dispersion*, when absorption is present, and if one limits the total propagation distance to just a few pulse widths, or distances smaller than typical bulk dispersion lengths. Restricting one's considerations to relatively small propagation distances that do not exceed a few pulse widths is usually more than sufficient in NIMS, for example, since the length of typical NIM structures realized to date is less than incident pulse spatial width [2–4]. These conditions are also easily satisfied if the pulse is incident on layered structures of finite extent, whose total thickness may be just a few wavelengths, and where geometrical dispersion (the presence of boundaries) tends to dominate over material dispersion, especially when index discontinuities are large [22]. These circumstances can be handily achieved in bulk materials that are well-described by the Drude model below the plasma frequency, metals for example. The Drude model is in fact widely used to describe and model NIMs. It is easy to verify that both the real and imaginary parts of the dielectric constant of silver (or other similar good conductor such as gold, copper or aluminum) [23] are *approximately* linear functions of frequency provided the range of interest is limited to just a few hundred nanometers at a time. This generally means that pulses just a few wave cycles in duration can easily satisfy our conditions at almost any carrier frequency, provided we do not allow the pulse to propagate too deep into the material. We will clarify and expand on the significance of this point in the next section, where we present the propagation model and give examples.

Because Eq. (1) is known to fail at least under certain conditions, we will attempt to derive a new generalized energy density that will replace it, and a new energy dissipation rate that will complement it. Then, we will derive equations of motion that describe the dynamics of pulses under condi-

tions of dispersive and discontinuous ε and μ, and we will see a novel effect emerge: as the pulse crosses the interface energy can be transferred from the electric to the magnetic field, or vice versa, depending on the chosen set of parameters. This effect cannot occur in ordinary materials ($\mu=1$). However, if the magnetic permeability is also discontinuous, but not necessarily negative, the energy content of the pulse is transformed.

II. ENERGY DENSITY AND ENERGY DISSIPATION RATES

Beginning from a dispersion relation, one usually needs to produce the time derivatives $\partial \mathbf{D}(\mathbf{r},t)/\partial t$ and $\partial \mathbf{B}(\mathbf{r},t)/\partial t$ from constitutive relations in order to write Maxwell's equations and proceed further. The alternative approach is to directly couple the material equations of motion for the polarization and magnetization to Maxwell's equations in the time domain [5,6,21]. In our view it is more instructive to proceed with constitutive relations for several related reasons: First, this approach leads to equations of motion that can be interpreted much more easily compared to other methods. Second, the resulting equations can effortlessly be extended to include an electric or magnetic nonlinearity, or both. Third, the method provides useful physical insight [24] into the dynamics unavailable with other methodologies, where for example the field equations are coupled with oscillator equations to yield a fully numerical approach [5]. Therefore, assuming the displacement vector $\mathbf{D}$ is linearly polarized along the x axis, we write it in complex notation in the usual manner: $\mathbf{D} = \mathbf{i}(D_x(\mathbf{r},t) + \text{c.c.})$. We now assume that the dispersion function can be written as a generic Taylor expansion/series as usual:

$$\varepsilon(\mathbf{r},\omega) = \varepsilon(\mathbf{r},\omega_0) + \left. \frac{\partial \varepsilon(\mathbf{r},\omega)}{\partial \omega} \right|_{\omega_0} (\omega - \omega_0)$$
$$+ \frac{1}{2} \left. \frac{\partial^2 \varepsilon(\mathbf{r},\omega)}{\partial \omega^2} \right|_{\omega_0} (\omega - \omega_0)^2 + \cdots$$
$$= a(\mathbf{r},\omega_0) + b(\mathbf{r},\omega_0)\omega + c(\mathbf{r},\omega_0)\omega^2 + \cdots. \quad (2)$$

For simplicity one may assume that ω_0 is the carrier frequency of the incident pulse. All coefficients are assumed to be complex, and their spatial dependence is meant to describe the presence of spatial inhomogeneities, such as physical boundaries, for example, although other types of anisotropies such as birefringence could also be taken into account. Then, the constitutive relation that ties the displacement vector to the electric field $\mathbf{E}(\mathbf{r},t) = \mathbf{i}[E_x(\mathbf{r},t) + \text{c.c.}]$ takes the form

$$D_x(\mathbf{r},t) = \int_{-\infty}^{\infty} \varepsilon(\mathbf{r},\omega) E_x(\mathbf{r},\omega) e^{-i\omega t} d\omega$$
$$= \int_{-\infty}^{\infty} \{a(\mathbf{r},\omega_0) + b(\mathbf{r},\omega_0)\omega + c(\mathbf{r},\omega_0)\omega^2 + \cdots\}$$
$$\times [E_x(\mathbf{r},\omega)] e^{-i\omega t} d\omega. \quad (3)$$

The integrations can be carried out exactly, and so we have

$$D_x(\mathbf{r},t) = a(\mathbf{r},\omega_0) E_x(\mathbf{r},t) + ib(\mathbf{r},\omega_0) \frac{\partial E_x(\mathbf{r},t)}{\partial t}$$
$$- c(\mathbf{r},\omega_0) \frac{\partial^2 E_x(\mathbf{r},t)}{\partial t^2} + \cdots. \quad (4)$$

Equivalent derivations [16,18] typically assume pulse envelopes to be slowly varying functions of time. Although Eq. (4) is an exact result that does not rely on slowly varying envelopes, it is nevertheless convenient and useful to separate the fields into an envelope function and a carrier frequency, making no assumptions about the field envelope. The decomposition can thus be regarded as a simple functional transformation. Then, assuming an electric field of the form $E_x(\mathbf{r},t) = \mathcal{E}_x(\mathbf{r},t) e^{-i\omega_0 t}$, it follows that

$$D_x(\mathbf{r},t) = a\mathcal{E}_x e^{-i\omega_0 t} + ib \left\{ \frac{\partial \mathcal{E}_x}{\partial t} - i\omega_0 \mathcal{E}_x \right\} e^{-i\omega_0 t}$$
$$- c \left\{ \frac{\partial^2 \mathcal{E}_x}{\partial t^2} - 2i\omega_0 \frac{\partial \mathcal{E}_x}{\partial t} - \omega_0^2 \mathcal{E}_x \right\} e^{-i\omega_0 t} + \cdots. \quad (5)$$

We have simplified the notation by dropping the explicit spatial and temporal dependence of all Taylor coefficients and $\mathcal{E}$. The calculation of $\partial D_x(\mathbf{r},t)/\partial t$ is straight forward, and the result is

$$\frac{\partial D_x(\mathbf{r},t)}{\partial t} = \left\{ -i\omega_0 \varepsilon(\omega_0) \mathcal{E}_x + \left[\frac{\partial[\omega\varepsilon(\omega)]}{\partial \omega} \right]_{\omega_0} \frac{\partial \mathcal{E}_x}{\partial t} \right. $$
$$\left. + \frac{i}{2} \left[\frac{\partial^2[\omega\varepsilon(\omega)]}{\partial \omega^2} \right]_{\omega_0} \frac{\partial^2 \mathcal{E}_x}{\partial t^2} + \cdots \right\} e^{-i\omega_0 t}, \quad (6)$$

which in turn can be expressed in a more compact form as [24]

$$\frac{\partial D_x(\mathbf{r},t)}{\partial t} = -\sum_{n=0}^{\infty} \left\{ i^{n+1} \left. \frac{\partial^n(\omega\varepsilon)}{\partial \omega^n} \right|_{\omega=\omega_0} \frac{1}{n!} \frac{\partial^2 \mathcal{E}_x}{\partial t^n} \right\} e^{-i\omega_0 t}. \quad (7)$$

Following the same procedure outlined between Eqs. (2)–(7), we can easily arrive at a similar expression for the magnetic field:

$$\frac{\partial B_y(\mathbf{r},t)}{\partial t} = -\sum_{n=0}^{\infty} \left\{ i^{n+1} \left. \frac{\partial^n(\omega\mu)}{\partial \omega^n} \right|_{\omega=\omega_0} \frac{1}{n!} \frac{\partial^2 \mathcal{H}_y}{\partial t^n} \right\} e^{-i\omega_0 t}. \quad (8)$$

At this point the derivation of Eq. (1) is typically carried out [16,18] by retaining only the first two leading terms in each of our Eqs. (7) and (8), and by neglecting absorption (both ε and μ are assumed to be real). The consequences of these choices lead to the restrictions that are implemented in [16,18], for example: (i) pulse bandwidth must be limited, i.e., pulses are quasimonochromatic, and/or (ii) both the dielectric susceptibility and the magnetic permeability *do not* display absorption, and (iii) are approximately linear functions of frequency; (iv) if broad bandwidth pulses are considered, then propagation distances should remain short, on the order of just a few pulse widths, so that higher order dispersive effects can still be neglected even if the dispersion functions display curvature within the bandwidth of the incident pulse. Instead, use of Eqs. (7) and (8) allows us to

immediately generalize Eq. (1) to the case where dispersion and absorption are present to an arbitrary degree. Substitution of Eqs. (7) and (8) into Poynting's theorem [16–18], namely $\partial U/\partial t + Q_{dissipated} = \mathbf{E} \cdot [\partial \mathbf{D}(\mathbf{r},t)/\partial t] + \mathbf{H} \cdot [\partial \mathbf{B}(\mathbf{r},t)/\partial t] = -\nabla \cdot \mathbf{S}$, results in the following expression:

$$\frac{\partial U}{\partial t} = \alpha_r \left(\mathcal{E}_x \frac{\partial \mathcal{E}_x^*}{\partial t} + \mathcal{E}_x^* \frac{\partial \mathcal{E}_x}{\partial t} \right) + \frac{i\alpha_r'}{2} \left(\mathcal{E}_x^* \frac{\partial^2 \mathcal{E}_x}{\partial t^2} - \mathcal{E}_x \frac{\partial^2 \mathcal{E}_x^*}{\partial t^2} \right)$$

$$+ \frac{\alpha_r''}{6} \left(\mathcal{E}_x \frac{\partial^3 \mathcal{E}_x^*}{\partial t^3} + \mathcal{E}_x^* \frac{\partial^3 \mathcal{E}_x}{\partial t^3} \right) + \gamma_r \left(\mathcal{H}_y \frac{\partial \mathcal{H}_y^*}{\partial t} + \mathcal{H}_y^* \frac{\partial \mathcal{H}_y}{\partial t} \right)$$

$$+ \frac{i\gamma_r'}{2} \left(\mathcal{H}_y^* \frac{\partial^2 \mathcal{H}_y}{\partial t^2} - \mathcal{H}_y \frac{\partial^2 \mathcal{H}_y^*}{\partial t^2} \right)$$

$$+ \frac{\gamma_r''}{6} \left(\mathcal{H}_y \frac{\partial^3 \mathcal{H}_y^*}{\partial t^3} + \mathcal{H}_y^* \frac{\partial^3 \mathcal{H}_y}{\partial t^3} \right) + \cdots . \tag{9}$$

Integration by parts and retention of just a few leading terms leads to the following modified, instantaneous energy density:

$$U(z,t) = \alpha_r |\mathcal{E}_x|^2 + \beta_r |\mathcal{H}_y|^2 + \frac{i\alpha_r'}{2} \left\{ \mathcal{E}_x^* \frac{\partial \mathcal{E}_x}{\partial t} - \mathcal{E}_x \frac{\partial \mathcal{E}_x^*}{\partial t} \right\}$$

$$+ \frac{i\beta_r'}{2} \left\{ \mathcal{H}_y^* \frac{\partial \mathcal{H}_y}{\partial t} - \mathcal{H}_y \frac{\partial \mathcal{H}_y^*}{\partial t} \right\}$$

$$+ \frac{\alpha_r''}{6} \left\{ \mathcal{E}_x \frac{\partial^2 \mathcal{E}_x^*}{\partial t^2} + \mathcal{E}_x^* \frac{\partial^2 \mathcal{E}_x}{\partial t^2} - \frac{\partial \mathcal{E}_x}{\partial t} \frac{\partial \mathcal{E}_x^*}{\partial t} \right\}$$

$$+ \frac{\gamma_r''}{6} \left\{ \mathcal{H}_y \frac{\partial^2 \mathcal{H}_y^*}{\partial t^2} + \mathcal{H}_y^* \frac{\partial^2 \mathcal{H}_y}{\partial t^2} - \frac{\partial \mathcal{H}_y}{\partial t} \frac{\partial \mathcal{H}_y^*}{\partial t} \right\} + \cdots \tag{10}$$

and to a corresponding expression for energy dissipation rate:

$$-Q_{dissipated}(z,t)$$

$$= 2\omega_0 \{ \varepsilon_i |\mathcal{E}_x|^2 + \mu_i |\mathcal{H}_y|^2 \} + i\alpha_i \left(\mathcal{E}_x^* \frac{\partial \mathcal{E}_x}{\partial t} - \mathcal{E}_x \frac{\partial \mathcal{E}_x^*}{\partial t} \right)$$

$$+ i\beta_i \left(\mathcal{H}_y^* \frac{\partial \mathcal{H}_y}{\partial t} - \mathcal{H}_y \frac{\partial \mathcal{H}_y^*}{\partial t} \right) - \frac{\alpha_i'}{2} \left(\mathcal{E}_x^* \frac{\partial^2 \mathcal{E}_x}{\partial t^2} + \mathcal{E}_x \frac{\partial^2 \mathcal{E}_x^*}{\partial t^2} \right)$$

$$- \frac{\beta_i'}{2} \left(\mathcal{H}_y^* \frac{\partial^2 \mathcal{H}_y}{\partial t^2} + \mathcal{H}_y \frac{\partial^2 \mathcal{H}_y^*}{\partial t^2} \right) + \cdots , \tag{11}$$

where $\alpha = \alpha_r + i\alpha_i = \partial[\omega\varepsilon(\omega)]/\partial\omega$, $\beta = \beta_r + i\beta_i = \partial[\omega\mu(\omega)]/\partial\omega$, and the prime symbol indicates differentiation with respect to the frequency. The leading terms in both Eqs. (10) and (11) can be identified as the energy density—Eq. (1)—and the corresponding energy absorption rate, respectively, for quasi-monochromatic pulses [16,18].

Equations (10) and (11) have general validity and are independent of any propagation model because the only assumptions that have been made in deriving them are that (i) a Taylor expansion can be used to describe both ε and μ; (ii) the real parts of ε and μ, and their derivatives, can be associated with energy flow, and that the corresponding imagi-

nary parts can be interpreted as energy dissipation rates in the usual way [16,18]. One should be mindful of the fact that the RHS of both Eqs. (10) and (11) may converge slowly, especially near resonances where dispersion is anomalous, large absorption is present, and functions may vary rapidly. Therefore, an unspecified number of terms beyond those shown may have to be included, depending on the slopes of ε and μ and on pulse duration. If we now write the field envelope as the product of an amplitude and a phase factor, both as functions of space and time, i.e., $\mathcal{E}(\mathbf{r},t) = |\mathcal{E}| e^{i\varphi_{\mathcal{E}}}$ and similarly for $\mathcal{H}$, and retaining just the first two electric and magnetic leading terms, Eqs. (10) and (11) can be recast in a different but equally suggestive form:

$$U(z,t) \approx (\alpha_r - \alpha_r' \dot\varphi_{\mathcal{E}}) |\mathcal{E}_x|^2 + (\beta_r - \beta_r' \dot\varphi_{\mathcal{H}}) |\mathcal{H}_y|^2 + \cdots \tag{12}$$

and

$$-Q_{dissipated}(z,t) \approx 2(\varepsilon_i \omega_0 - \alpha_i' \dot\varphi_{\mathcal{E}}) |\mathcal{E}_x|^2 + 2(\mu_i \omega_0 - \gamma_i' \dot\varphi_{\mathcal{H}})$$

$$\times |\mathcal{H}_y|^2 + \cdots . \tag{13}$$

These equations illustrate that in general the *evolution and signs* of the phases of the fields are just as important as the slopes of ε and μ, even if $\varphi_{\mathcal{E}}$ and $\varphi_{\mathcal{H}}$ are relatively slowly varying functions of time.

III. EQUATIONS OF MOTION AND PROPAGATION MODEL

We are now interested in deriving a set of equations that describes the dynamics of a pulse crossing an interface between two arbitrary media, where at least one of them is magnetically active, in order to accurately describe the scattering event. As we do this we will see a different effect take shape: energy can flow from the electric field to the magnetic field, or vice versa. To facilitate our task we make a simple, practical but not too restrictive assumption: we limit the total propagation distance inside the magnetically active material to just a few pulse widths, regardless of pulse duration. This allows us to truncate the Taylor expansion in Eq. (2) at the second term, in effect rendering Eqs. (12) and (13) nearly exact for almost any pulse that has crossed but is still located relatively near the surface. Of course, relatively long pulses whose duration is several tens of wave cycles in duration can propagate further without incurring significant error.

The treatment of all orders of dispersion for bulk propagation becomes necessary should propagation distances become large, and can always be done in other ways, for example by deriving a Schrödinger equation for the case of magnetically active materials [24]. Alternatively, if higher orders of dispersion are a real concern, one may preempt them by tuning the carrier frequency of very short pulses (on the order of the wave period) at frequencies where the group velocity dispersion coefficient crosses the axis [25], thus diminishing the importance of higher order temporal derivatives. In other words, these arguments amount to saying that higher order dispersion terms may generally be neglected because the corresponding dispersion lengths may be at least
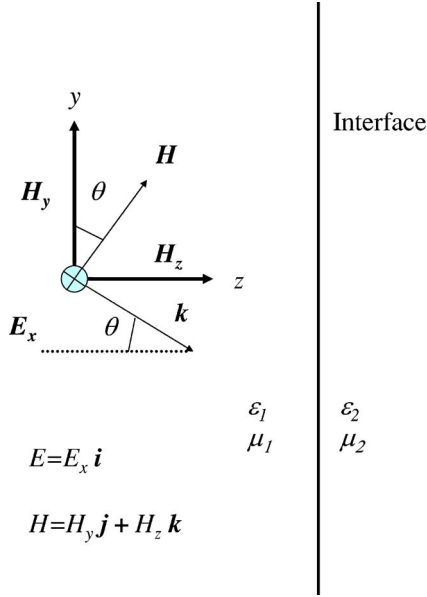
FIG. 1. (Color online) A pulse is initially located on the left side of an interface which separates two generic media. The electric field is polarized into the page. At oblique incidence this setup yields two magnetic field components, one transverse and one longitudinal with respect to the direction of propagation. The model can easily be adjusted to include incident TM polarized pulses, and can also easily be extended to a full 3D model.

several tens of pulse widths, and thus do not affect the dynamics we are studying. Consequently, we properly and correctly monitor the pulse group and energy velocities at all times even when we treat short pulses. The neglect of curvature effects, and group velocity dispersion along with it, may become a concern should pulse duration become too short, and/or if propagation distances inside a uniform medium become considerable (several tens of pulse widths).

With these considerations in mind, we assume a pulse is initially located in vacuum, some distance away from an interface that separates two generic materials. The electric field is linearly polarized, points into the page, and is incident at an arbitrary angle θ_i, as shown in Fig. 1. We expand the fields as follows:

$$\mathbf{E} = \mathbf{i}[\mathcal{E}_x(y,z,t)e^{i(k_z z - k_y y - \omega t)} + \text{c.c.}],$$

$$\mathbf{H} = \mathbf{j}[\mathcal{H}_y(y,z,t)e^{i(k_z z - k_y y - \omega t)} + \text{c.c.}]$$
$$+ \mathbf{k}[\mathcal{H}_z(y,z,t)e^{i(k_z z - k_y y - \omega t)} + \text{c.c.}], \tag{14}$$

where $k_z = |\mathbf{k}|\cos\theta_i$ and $k_y = -|\mathbf{k}|\sin\theta_i$, $|\mathbf{k}| = k_0 = \omega/c$. This choice of carrier wave vector is consistent with the fact that the pulse is initially located in vacuum, but one can easily introduce another background index. We make no other assumptions about the envelope functions, and the fields' phases are allowed to evolve free of preconditions, as functions of position and time. We substitute Eqs. (7), (8), and (14) into the vector Maxwell equations:

$$\nabla \times \mathbf{E} = -\frac{1}{c}\frac{\partial \mathbf{B}}{\partial t},$$

$$\nabla \times \mathbf{H} = \frac{1}{c}\frac{\partial \mathbf{D}}{\partial t}. \tag{15}$$

Retaining only the first two leading terms on the RHS of Eqs. (7) and (8) to reflect our assumption of approximately linear ε and μ, and rearranging terms, we obtain a set of three coupled equations for the field envelopes [26]:

$$\frac{\partial[\tilde{\omega}\varepsilon(\xi)]}{\partial\tilde{\omega}}\frac{\partial\mathcal{E}_x}{\partial\tau} = i\beta[\varepsilon(\xi)\mathcal{E}_x - \mathcal{H}_z\sin\theta_i - \mathcal{H}_y\cos\theta_i]$$
$$+ \frac{\partial\mathcal{H}_z}{\partial\tilde{y}} - \frac{\partial\mathcal{H}_y}{\partial\xi},$$

$$\frac{\partial[\tilde{\omega}\mu(\xi)]}{\partial\tilde{\omega}}\frac{\partial\mathcal{H}_y}{\partial\tau} = i\beta[\mu(\xi)\mathcal{H}_y - \mathcal{E}_x\cos\theta_i] - \frac{\partial\mathcal{E}_x}{\partial\xi},$$

$$\frac{\partial[\tilde{\omega}\mu(\xi)]}{\partial\tilde{\omega}}\frac{\partial\mathcal{H}_z}{\partial\tau} = i\beta[\mu(\xi)\mathcal{H}_z - \mathcal{E}_x\sin\theta_i] + \frac{\partial\mathcal{E}_x}{\partial\tilde{y}}. \tag{16}$$

The following scaling has been adopted: $\xi = z/\lambda_p$, $\tilde{x} = x/\lambda_p$; $\tau = ct/\lambda_p$, $\beta = 2\pi\tilde{\omega}$, and $\tilde{\omega} = \omega/\omega_p$, where λ_p is conveniently chosen to be the wavelength associated with the plasma frequency. Writing the propagation equations as they appear in Eqs. (16) provides insight that is normally absent when one pursues a fully numerical approach. For instance, the form of the equations immediately suggests a positive group velocity for propagation in uniform, relatively transparent media, based on the fact that energy should be positive [16]: $1/V_g \approx \sqrt{(\partial[\tilde{\omega}\varepsilon(\xi)]/\partial\tilde{\omega})(\partial[\tilde{\omega}\mu(\xi)]/\partial\tilde{\omega})}$. One may show this by eliminating the H field and by writing the wave equation for the electric field, for instance [24]. For the interested reader, there is an extended discussion of wave packet dynamics, including chirp, spatial pulse compression, and the study of conjugate space in Ref. [26], were Eqs. (16) are also derived and solved the same way. In summary, to arrive at Eqs. (16) we have assumed that ε and μ are complex and approximately linear in the region of interest. The equations are then solved in the time domain using a modified fast Fourier transform pulse propagation method designed to handle arbitrary spatial discontinuities [27]. The method of integration is unconditionally stable [28], converges rapidly, and its implementation involves simple multiplication of linear operators [27].

IV. PROPAGATION INTO A NIM

We now illustrate the dynamics with a representative example. At normal incidence, assuming infinite Fresnel number (transverse profile of the pulse is wide enough so that it does not diffract over the propagation distances involved), Eqs. (16) reduce to a set of two coupled equations, namely [26]
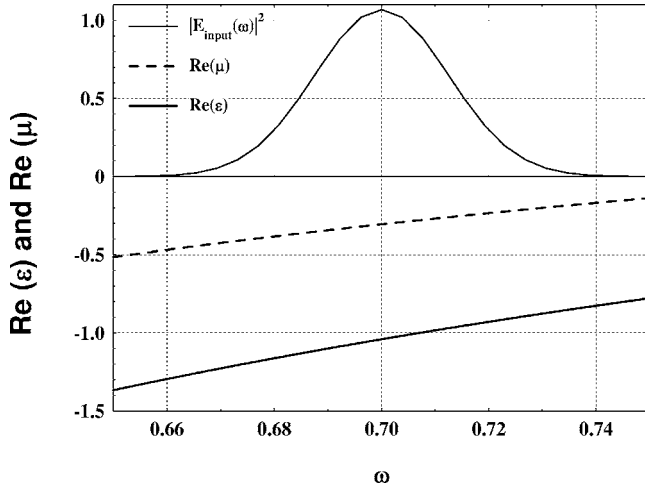
FIG. 2. Re(ε) (solid), Re(μ) (dashed) versus normalized frequency, and spectrum of an 80-wave cycle incident pulse, which we define as follows: $E(\xi,0)=E_0 e^{-(\xi^2/80^2)}$.

$$\frac{\partial[\tilde{\omega}\varepsilon(\xi)]}{\partial\tilde{\omega}}\frac{\partial\mathcal{E}_x}{\partial\tau} = i\beta[\varepsilon(\xi)\mathcal{E}_x - \mathcal{H}_y] - \frac{\partial\mathcal{H}_y}{\partial\xi},$$

$$\frac{\partial[\tilde{\omega}\mu(\xi)]}{\partial\tilde{\omega}}\frac{\partial\mathcal{H}_y}{\partial\tau} = i\beta[\mu(\xi)\mathcal{H}_y - \mathcal{E}_x] - \frac{\partial\mathcal{E}_x}{\partial\xi}. \quad (17)$$

Although the parameters we use are consistent with a Drude model described by $\varepsilon(\tilde{\omega})=1-1/(\tilde{\omega}^2+i\tilde{\omega}\gamma)$, and $\mu(\tilde{\omega})=1-(\omega_m^2/\omega_p^2)/(\tilde{\omega}^2+i\tilde{\omega}\gamma)$, the qualitative and quantitative results are valid for a general class of dispersion models. We choose an incident pulse with carrier frequency tuned at $\tilde{\omega}=0.7$, approximately 80 wave cycles in duration, and both ε and μ are negative. We note that causality here demands only that $\gamma\neq 0$, and so in our first example we choose $\gamma=5\times 10^{-5}$, which results in a complex index of refraction (at the carrier frequency) $n=-0.564+i1.25\times 10^{-4}$, and a relatively small but measurable absorption.

In Fig. 2 we show Re(ε) (thick solid line) and Re(μ) (thick dashed line) for $\omega_m^2/\omega_p^2=0.64$. In the same figure we also show the bandwidth of the incident pulse (thin solid line). It is evident that both ε and μ are approximately linear functions of frequency in the range of interest, and so the propagation of this pulse is described very well by Eqs. (16) and (17) for quite some distance inside the material. In fact, the second and third order dispersion lengths can be estimated using the simple relationships $L_D^{(2)}\sim\tau_p^2/|k''|$ and $L_D^{(3)}\sim\tau_p^3/|k'''|$, where τ_p is the initial pulse duration, and k'' and k''' are second and third order dispersion coefficients. For the pulse and the dispersion functions of Fig. 2, at $\tilde{\omega}=0.7$ and $\tau_p\sim 80\lambda_p$; $|k''|\sim 0.1$; $|k'''|\sim 2.5$, the respective dispersion lengths are $L_D^{(2)}\sim 6.4\times 10^4\lambda_p$ and $L_D^{(3)}\sim 2\times 10^5\lambda_p$ [24,25], respectively.

In Fig. 3 we show the input and output electric and magnetic field intensities corresponding to Fig. 2. Should the condition $\varepsilon=\mu$ be satisfied, regardless of their magnitudes, then $\mathcal{E}=\mathcal{H}$ everywhere away from the interface inside and outside the material. However, here the relative amplitudes
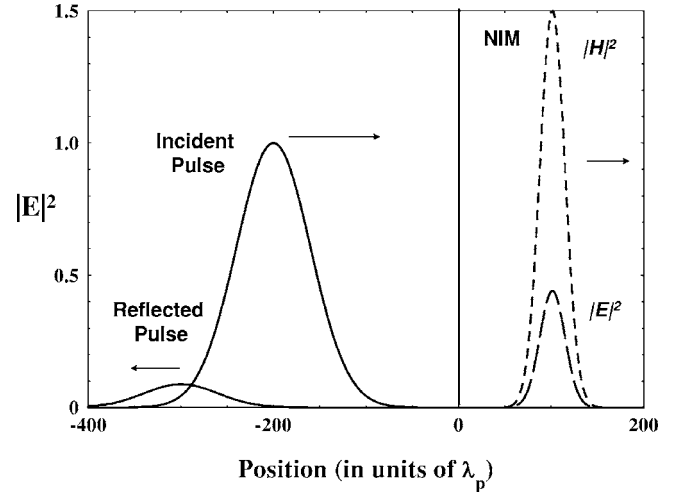

FIG. 3. Electric and magnetic field pulses that are incident, reflected, and transmitted from an interface that separates vacuum from a NIM. The incident pulse is that described in Fig. 2, with its carrier frequency tuned at $\tilde{\omega}=0.7$. The values of ε and μ are obtained using $\gamma=5\times 10^{-5}$ in the Drude dispersion: $\varepsilon=-0.104+i1.458\times 10^{-4}$ and $\mu=-0.306+i9.33\times 10^{-4}$, with corresponding values $\partial[\tilde{\omega}\varepsilon(\xi)]/\partial\tilde{\omega}|_{\tilde{\omega}=0.7}=3.04-i2.9\times 10^{-4}$ and $\partial[\tilde{\omega}\mu(\xi)]/\partial\tilde{\omega}|_{\tilde{\omega}=0.7}=2.3-i1.86\times 10^{-4}$. The integrations converge rapidly, and so it is sufficient to set $\delta\xi=\delta\tau=0.025$.

of $\mathcal{H}$ and $\mathcal{E}$ differ inside the material because $\varepsilon\neq\mu$, and reflected and transmitted amplitudes develop according to the boundary conditions.

We now come to the evaluation of Eqs. (10) and (11), or in the case of approximately linear dispersion (or equivalently, relatively short propagation distances), Eqs. (12) and (13). In Fig. 4 we plot the total energy, defined as $W_T(\tau)=\int_{-\infty}^{\infty}U(\xi,\tau)d\xi$, as the sum of the electric and magnetic energies, also shown individually, as functions of time. We find that energy actually flows from the electric to the mag-
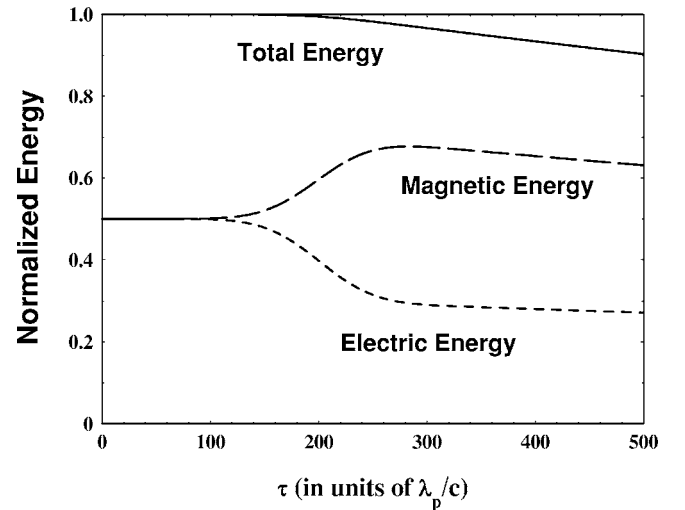

FIG. 4. Total, electric, and magnetic energies that result from the scattering of the pulses depicted in Fig. 3. The figure clearly shows that energy flows from the electric field to the magnetic field, an event that cannot occur for ordinary materials.

netic field as the pulse traverses the interface. In addition, one can arrange the parameters in such a way that energy flows from the magnetic to the electric field. Although we do not show this, this in fact occurs when we choose $\omega_m^2/\omega_p^2=1.44$, and tune the carrier frequency to $\tilde{\omega}=0.892$ ($n=-0.456+i9.11\times10^{-5}$): the relative magnitudes of ε and μ are inverted, yielding a process similar to what occurs in Fig. 4, only reversed in terms of $\mathcal{E}$ and $\mathcal{H}$. To our knowledge, this kind of energy exchange and its implications have not been investigated to any significant degree, probably because magnetic discontinuities were almost never an issue. In fact, for this process to occur we find that it is sufficient to have both ε and μ different and discontinuous, but not necessarily negative. For example, we obtain a figure once again similar to Fig. 4 by setting $\omega_m^2/\omega_p^2=1.44$ and $\tilde{\omega}=1.3$, which tunes the fields in a region of positive index: $n=0.246+i3.4\times10^{-5}$.

When a pulse crosses an ordinary dielectric interface ($n>1$ and $\mu=1$ everywhere) electric energy becomes temporarily stored in the medium, causing the amplitude of the electric field to decrease. At the same time, the pulse slows down and becomes spatially compressed by a factor roughly proportional to the group index. The magnetic field, on the other hand, cannot give up its energy directly to the medium due to the absence of magnetic dipoles, and so the spatial compression is usually accompanied by an increase of its maximum amplitude. Therefore, to the extent that absorption may be ignored, electric and magnetic energies must be *individually* conserved.

Once we allow for the presence of magnetic dipoles, the global requirement that energy be conserved [i.e., the sum of the two terms in Eq. (1)] does not necessarily extend to the individual electric and magnetic fields. As a result, while the boundary conditions establish the individual peak field amplitudes inside the medium, and the group index determines the pulse spatial compression factor [26], there is nothing to constrain electric dipoles from temporarily giving up energy so that more energy is stored in magnetic form. (In the case of pulses the boundary condition, which is of course defined and intended to apply to pure plane waves, should be interpreted as the peak value of a pulse that approaches quasimonochromatic status). The ability to shift energy from the electric to the magnetic field or vice versa may be important to highlight magnetic effects, and for nonlinear applications [12,13], where one field or the other may be favored [29], and thus thresholds lowered, if one field or the other can be used as a reservoir.

Returning to Fig. 4, it is evident that the total energy residing in the fields decreases as the pulse penetrates further into the medium and is transformed into heat. We now highlight qualitative and quantitative differences between Eq. (1) and Eq. (12) as a function of decreasing pulse duration, in the presence of considerable absorption, but by keeping dispersion approximately linear and/or by keeping propagation distance down to just a few pulse widths. This allows us to clearly focus on the pulse as it crosses the interface. In Fig. 5 we use the same parameters used in Fig. 4, except that now $\gamma=10^{-3}$ and $n=-0.5645+i2.51\times10^{-3}$, and plot the energy as given by Eqs. (1) and (12), for an incident pulse only 5 wave cycles in duration. The second and third order dispersion lengths are $L_D^{(2)}\sim\tau_p^2/|k''|\sim250\lambda_p$ and $L_D^{(3)}\sim\tau_p^3/|k'''|\sim50\lambda_p$,
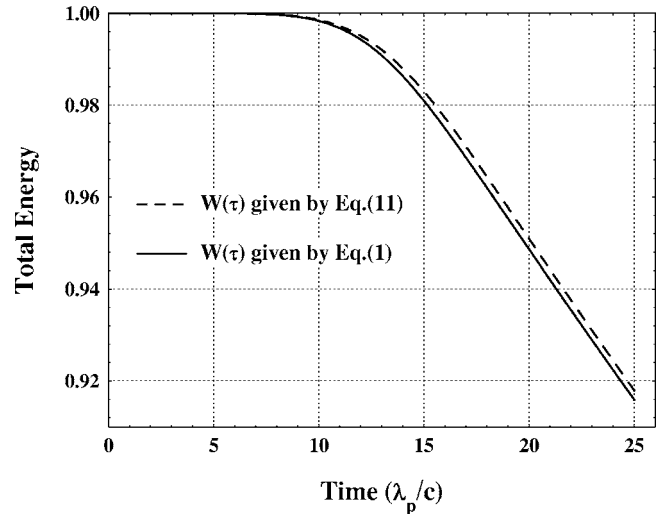

FIG. 5. Calculation of the total energy via Eq. (1) (solid line) and the new Eq. (11) for a pulse only 5 wave cycles in duration, $E(\xi,0)=E_0 e^{-(\xi^2/5^2)}$ under conditions of approximately linear dispersion. There is a small discrepancy of approximately 0.2% between the two curves, an indication that indeed Eq. (1) can accurately describe what happens to the energy of the pulse as it crosses an interface.

respectively [24,25]. An analysis of the data and the figure suggests that Eqs. (1) and (12) yield energies with a difference smaller than 0.2%. We record approximately the same difference for Q, the energy absorption rate corresponding to Eq. (1).

The results outlined above clearly suggest that if dispersion remained approximately linear, but arbitrarily large (neglecting curvature in the dispersion functions *does not* mean one is neglecting dispersion. Indeed, the slope of the dispersion functions may be quite steep even in the absence of curvature; this is all that the model requires) then the error incurred in using Eq. (1) rather than Eq. (12) appears to be approximately 0.2%, even for pulses that are only a few wave cycles in duration. In reality we expect that the linear dispersion model will begin to fail for pulses that are longer than the 5 wave cycles that we used, as pulse bandwidth begins to spill over into regions where curvature cannot be neglected, even for short propagation distances.

A more precise assessment of the error incurred can be made through an independent verification of Poynting's theorem, which amounts to a statement of conservation of energy: it is required that the rate of change of energy flow within a certain region of space must equal the rate at which energy is being absorbed within that same volume, namely

$$\int_{-\infty}^{\infty}d\xi\frac{\partial U(\xi,\tau)}{\partial\tau}=\frac{\partial W_T(\tau)}{\partial\tau}=-\int_{-\infty}^{\infty}d\xi\,Q(\xi,\tau). \qquad (18)$$

The circulation of the Poynting vector vanishes when the integral is evaluated over all space. We have assumed that any shape changes along the transverse coordinates can be ignored, but for energy considerations the integrations along x and y in Eq. (18) are of course implied. We therefore proceed as follows: we first calculate the total energy $W_T(\tau)$ and

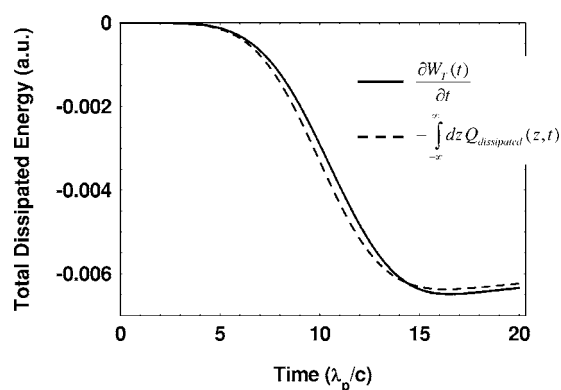FIG. 6. Dissipated energy as a function of time, for the same incident pulse of Fig. 5, $E(\xi,0)=E_0 e^{-(\xi^2/5^2)}$, calculated via the derivative of the total energy (solid curve), and via the integration of Eq. (12) (dashed curve). The difference between the two curves is approximately 1.4%. Once again, this confirms that the approximately linear dispersion model remains viable even for very short pulses.

its derivative, and then compare the result with the direct integration of Eq. (13), namely $-\int_{-\infty}^{\infty} d\xi Q_{dissipated}(\xi,\tau)$. The results of this procedure are depicted in Fig. 6, where we plot typical $\partial W_T(\tau)/\partial \tau$ (solid) and $-\int_{-\infty}^{\infty} d\xi Q_{dissipated}(\xi,\tau)$ (dashed) curves. The figure reveals that the discrepancy is approximately 1.4% for pulses 5 wave cycles in duration, and about 0.5% for 15-wave cycle pulses (not shown). Therefore, we conclude that for all practical purposes, the approximately linear dispersion model is more than adequate to study the dynamics of almost any pulse that transits across an interface. To take the pulse further into the medium, one can always add dispersive terms to Eqs. (16) and (17), or integrate the equations of motion including all orders of dispersion using any of a number of techniques [5,24,28]. However, the energy exchange process that we have described above occurs as the pulse crosses the surface, and the model exemplified by Eqs. (16) is more than adequate for that purpose.

Finally in Fig. 7 we show the typical result of integrating Eqs. (16) for an obliquely incident Gaussian pulse approximately 20 wave cycles in duration, located in vacuum, that crosses into a NIM for the parameters of Fig. 5. The figure shows a series of snapshots that mark the pulse location in space as the interaction proceeds. Each arrow clearly indicates the direction of the incident, transmitted, and reflected wave packets. We note that the transmitted pulse refracts negatively and is quickly being absorbed.
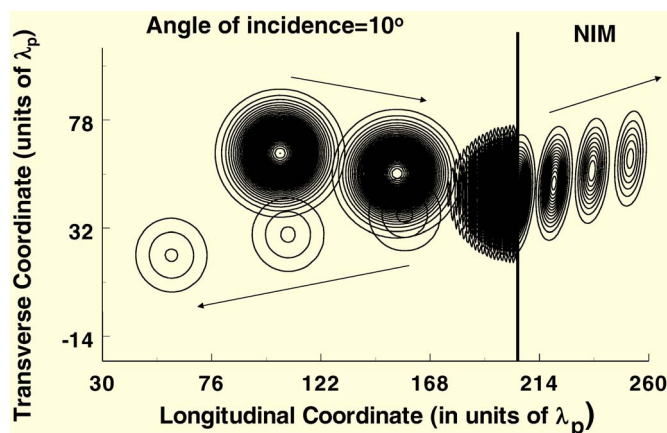

FIG. 7. (Color online) Negative refraction of an incident pulse approximately 20 wave cycles in duration: $E(\xi,y,\tau=0)=E_0 e^{-(\xi^2+y^2)/20^2}$. The results are consistent with what is found in the literature. The transverse coordinate may be discretized much less finely compared to the longitudinal coordinate, as there are no transverse boundaries to cross. Typically, $\delta x \sim \lambda$.

V. CONCLUSIONS

We integrate equations of motion that describe the dynamics of electromagnetic pulses transiting into magnetic materials (see also Ref. 26), and used them to show that a new effect occurs as the pulse traverses the surface boundary: energy can be transferred from the electric to the magnetic field or vice versa. This dynamics is fully consistent with the global requirement that the total energy should be conserved. We have also derived new generalized expressions for energy density and energy dissipation rates assuming the dispersion functions can be represented as a Taylor expansion, which includes all analytic functions. We have also verified that, under conditions of normal dispersion, the energy density commonly used to describe the energy density of quasi-monochromatic pulses in the absence of absorption can still be used for pulses that are just a few wave cycles in duration, when absorption is arbitrarily (but causally) large. We limit total propagation distance into the medium to just a few pulses widths, which is quite adequate for NIMs or for studying surface effects. The model is also particularly useful to describe pulse propagation effects in finite, layered structures with large index discontinuities, as their typical lengths are only a small fraction of the corresponding spatial extent of the pulse [22].

[1] V. G. Veselago, Sov. Phys. Usp. **10**, 509 (1968).

[2] R. A. Shelby, D. A. Smith, and S. Schultz, Science **292**, 77 (2001); C. G. Parazzoli *et al.*, Phys. Rev. Lett. **90**, 107401 (2003).

[3] J. B. Pendry, A. J. Holden, D. J. Robbins, and W. J. Stewart, IEEE Trans. Microwave Theory Tech. **47**, 2075 (1999); J. B. Pendry, Phys. Rev. Lett. **85**, 3966 (2000).

[4] D. R. Smith and N. Kroll, Phys. Rev. Lett. **85**, 2933 (2000); R. W. Ziolkowski and A. D. Kipple, Phys. Rev. E **68**, 026615 (2003); R. W. Ziolkowski and E. Heyman, Phys. Rev. E **64**, 056625 (2001).

[5] R. W. Ziolkowski, Phys. Rev. E **64**, 046604 (2001); S. D.

Gupta, R. Arun, and G. S. Agarwal, Phys. Rev. B **69**, 113104 (2004).

[6] R. W. Ziolkowski, Opt. Express **11**, 662 (2003).

[7] D. R. Smith, D. Schurig, and J. B. Pendry, Appl. Phys. Lett. **81**, 2713 (2002); S. Cummer, Appl. Phys. Lett. **82**, 2008 (2003).

[8] P. W. Milonni and G. J. Maclay, Opt. Commun. **228**, 161 (2003).

[9] D. R. Fredkin and A. Ron, Appl. Phys. Lett. **81**, 1753 (2002).

[10] V. M. Agranovich, Y. R. Shen, R. H. Baughman, and A. A. Zakhidov, Phys. Rev. B **69**, 165112 (2004).

[11] I. V. Shadrivov, A. A. Sukhorukov, and Y. S. Kivshar, Phys. Rev. E **67**, 057602 (2003).

[12] G. D'Aguanno, N. Mattiucci, M. Scalora, and M. J. Bloemer, Phys. Rev. Lett. **93**, 213902 (2004).

[13] M. W. Feise, I. V. Shadrivov, and Y. S. Kivshar, Phys. Rev. E **71**, 037602 (2005).

[14] W. T. Lu, J. B. Sokoloff, and S. Sridhar, Phys. Rev. E **69**, 026604 (2004).

[15] X. Huang and W. L. Schaich, Am. J. Phys. **72**, 1232 (2004).

[16] L. D. Landau and E. M. Lifshitz, *Electrodynamics of Continuous Media* (Pergamon, New York, 1960), pp. 253–256.

[17] J. D. Jackson, *Classical Electrodynamics*, 2nd ed. (Wiley, New York, 1975), Chap. 6.

[18] Y. R. Shen, *The Principles of Nonlinear Optics* (Wiley, New York, 1984).

[19] J. Askne and B. Lind, Phys. Rev. A **2**, 2335 (1970).

[20] V. L. Ginzburg, *The Propagation of Electromagnetic Waves* (Pergamon Press, Oxford, 1964).

[21] T. J. Cui and J. A. Kong, Phys. Rev. B **70**, 205106 (2004).

[22] M. Centini, C. Sibilia, M. Scalora, G. D'Aguanno, M. Bertolotti, M. J. Bloemer, C. M. Bowden, and I. Nefedov, Phys. Rev. E **60**, 4891 (1999); M. Centini, M. J. Bloemer, K. Myneni, M. Scalora, C. Sibilia, M. Bertolotti, and G. D'Aguanno, Phys. Rev. E **68**, 016602 (2003); G. D'Aguanno, M. Centini, M. J. Bloemer, K. Myneni, M. Scalora, C. M. Bowden, C. Sibilia, and M. Bertolotti, Opt. Lett. **27**, 176 (2002); M. J. Bloemer, K. Myneni, M. Centini, M. Scalora, and G. D'Aguanno, Phys. Rev. E **65**, 056615 (2002).

[23] *Handbook of Optical Constants of Solids*, edited by E. D. Palik (Academic, New York, 1985).

[24] M. Scalora, M. Syrchin, N. Akozbek, E. Y. Poliakov, G. D'Aguanno, N. Mattiucci, M. J. Bloemer, and A. M. Zheltikov, Phys. Rev. Lett. **95**, 013902 (2005).

[25] G. D'Aguanno, N. Akozbek, N. Mattiucci, M. Scalora, M. J. Bloemer, and A. M. Zheltikov, Opt. Lett. **30**, 1998 (2005).

[26] M. Scalora, G. D'Aguanno, N. Mattiucci, M. J. Bloemer, J. W. Haus, and A. M. Zheltikov, Appl. Phys. B: Lasers Opt. **81**, 393 (2005).

[27] M. Scalora and M. E. Crenshaw, Opt. Commun. **108**, 191 (1994).

[28] W. H. Press, S. A. Teukolsky, W. T. Vetterling, and B. P. Flannery, *Numerical Recipes in C: The Art of Scientific Computing*, 2nd ed. (Cambridge University Press, Cambridge, UK, 1997).

[29] A. A. Zharov, I. V. Shadrivov, and Y. S. Kivshar, Phys. Rev. Lett. **91**, 037401-1 (2003).